Redox Thermodynamics of the Fe(III)/Fe(II) Couple of Human Myeloperoxidase in Its High-Spin and Low-Spin Forms†

Gianantonio Battistuzzi,*,‡ Marzia Bellei,‡ Martina Zederbauer,§ Paul G. Furtmüller,§ Marco Sola,‡ and Christian Obinger*,§

Department of Chemistry, University of Modena and Reggio Emilia, via Campi 183, 41100 Modena, Italy, and Department of Chemistry, Division of Biochemistry, BOKU, University of Natural Resources and Applied Life Sciences, Muthgasse 18, A-1190 Vienna, Austria

Received August 14, 2006; Revised Manuscript Received September 4, 2006

ABSTRACT: Myeloperoxidase (MPO) (donor, hydrogen peroxide oxidoreductase, EC 1.11.1.7) is the most abundant neutrophil enzyme and catalyzes predominantly the two-electron oxidation of ubiquitous chloride (Cl^-), to generate the potent bleaching oxidant hypochlorous acid (HOCl), thus contributing to bacterial killing and inflammatory reactions of neutrophils. Here, the thermodynamics of the one-electron reduction of the ferric heme in its ferric high-spin and cyanide-bound low-spin forms were determined through spectroelectrochemical experiments. The $E°'$ values for free and cyanide-bound MPO (5 and −37 mV, respectively, at 25 °C and pH 7.0) are significantly higher than those of other heme peroxidases. Variable-temperature experiments revealed that the enthalpic stabilization of ferric high-spin MPO is much weaker than in other heme peroxidases and is exactly compensated by the entropic change upon reduction. In contrast to those of other heme peroxidases, the stabilization of the ferric cyanide-bound MPO is also very weak and fully entropic. This peculiar behavior is discussed with respect to the MPO-typical covalent heme to protein linkages as well as to the published structures of ferric MPO and its cyanide complex and the recently published structure of lactoperoxidase as well as the physiological role of MPO in bacterial killing.

Myeloperoxidase (MPO)[1] is a heme-containing dominant granule enzyme present in circulating polymorphonuclear neutrophils, which represent the cornerstone of cell-mediated antimicrobial activity in the human innate immune system (*1*). The principal reaction catalyzed by MPO under physiological conditions is thought to be the oxidation of chloride by H_2O_2 which yields the highly reactive oxidizing and chlorinating agent hypochlorous acid (HOCl) (*1*). In this respect, MPO is unique among the other members of the animal peroxidase superfamily (*2*) because its redox intermediate compound I possesses sufficient oxidation capacity to oxidize chloride in a two-electron reaction (*3*). Hypochlorous acid can participate in subsequent nonenzymatic reactions such as oxidation and chlorination of target-cell components.

The structure of MPO has been determined. Crystal structures are available for the ferric protein (*4*) and for its complex with cyanide and bromide (*5*). The ferric protein contains a water molecule weakly bound to the heme iron, which is displaced by a cyanide in the corresponding adduct (Figure 1). In MPO, the heme is covalently attached to the protein via two ester linkages between the carboxyl groups of Glu242 and Asp94 and modified methyl groups on pyrrole rings A and C of the heme (positions 1 and 5, respectively) as well as a sulfonium linkage between the sulfur atom of Met243 and the β-carbon of the vinyl group on pyrrole ring A (position 2) (Figure 1). Due to the covalent bonds, the heme ring assumes a bow-shaped structure. In fact, although pyrrole rings B and D are nearly coplanar, rings A and C are tilted toward the distal side (Figure 1A,C).

In all other members of the animal heme peroxidase superfamily [e.g., lactoperoxidase (LPO), eosinophil peroxidase (EPO), and thyroid peroxidase (TPO)], the heme is covalently linked by only two ester bonds. The heme in LPO is less distorted compared to that in MPO as the recently published structure in the Protein Data Bank (entry 2GJ1) demonstrates. It is thought that these differences in heme linkage could be a major factor that contributes to the differences in optical properties as well as substrate specificity of the heme enzymes (*6*−*10*).

Closely related to the mode of heme to protein linkages are the redox properties of MPO. Normally, in heme peroxidases, the Fe(III)/Fe(II) reduction potential ranges between −180 and −300 mV (*11*), which guarantees a stable

† This work was supported by the Ministero dell'Universita e della Ricerca Scientifica e Tecnologica of Italy and Fondazione di Risparmio di Modena 16/4/2002 and the Austrian Science Fund (Project P15660).

* To whom correspondence should be addressed. G.B.: e-mail, gianantonio.battistuzzi@unimore.it; phone, +39-59-2055117; fax, +39-59-3735543. C.O.: e-mail, christian.obinger@boku.ac.at; phone, +43-1-36006-6073; fax, +43-1-36006-6059.

‡ University of Modena and Reggio Emilia.

§ University of Natural Resources and Applied Life Sciences.

[1] Abbreviations: MPO, myeloperoxidase; LPO, lactoperoxidase; EPO, eosinophil peroxidase; TPO, thyroid peroxidase; ARP, *Athromyces ramosus* peroxidase; HRP-C, horseradish peroxidase isoform C; $E°'$, reduction potential, termed the standard hydrogen electrode, measured at pH 7.0; $\Delta H°'_{rc}$, enthalpy change for the reaction center upon reduction of the oxidized protein; $\Delta S°'_{rc}$, entropy change for the reaction center upon reduction of the oxidized protein; SHE, standard hydrogen electrode; ET, electron transport.

10.1021/bi061647k CCC: $33.50
Published on Web 10/03/2006

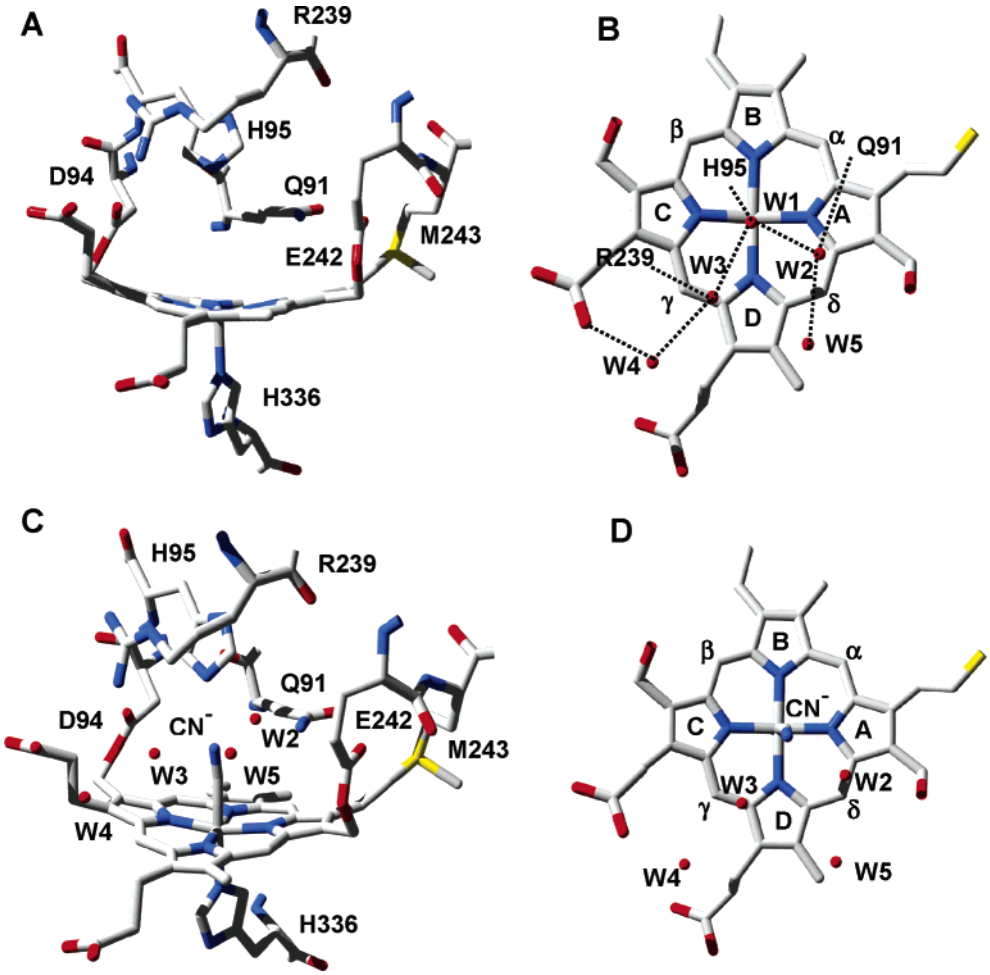

FIGURE 1: (A) Nonplanar porphyrin ring in MPO and its covalent attachments to the protein via two ester bonds (Asp94 and Glu242) and one sulfonium linkage (Met243). In addition, catalytic residues His95, Arg239, and Gln91 are shown, the latter being important in halide binding. (B) Locations of the five water molecules in the distal heme cavity of ferric high-spin MPO. This panel was constructed using the coordinates deposited in the Protein Data Bank (entry 1CXP). (C) Structure of the myeloperoxidase−cyanide complex. (D) View approximately normal to the heme plane. This panel was constructed using the coordinates deposited in the Protein Data Bank (entry 1D5L).

Fe(III) form under physiological conditions. Only the ferric form can be efficiently oxidized by H_2O_2 to the redox intermediate compound I, which finally oxidizes a variety of organic and inorganic substrates in either one- or two-electron oxidation reactions. The midpoint potential ($E^{\circ\prime}$) of the ferric/ferrous couple of bovine LPO was determined to be −190 mV (*12*). By contrast, the corresponding couple of MPO was reported to be 21 mV (*13*, *14*), similar to those of globins (myoglobin and hemoglobin), which have to be stable in the ferrous form to function as reversible oxygen carriers. With respect to that, MPO is a peculiar peroxidase, and an understanding of the functional consequences needs the analysis of the influences of protein matrix and solvent organization on the electronic structure of MPO.

Valuable information about the mechanism of $E^{\circ\prime}$ modulation in heme proteins has been obtained from the enthalpy ($\Delta H^{\circ\prime}_{rc}$) and entropy ($\Delta S^{\circ\prime}_{rc}$) changes of the reduction reaction, measured through variable-temperature electrochemical and spectroelectrochemical experiments (*15*−*21*). This paper reports for the first time on the thermodynamics of Fe(III) to Fe(II) reduction for the high-spin and cyanide-bound form of a member of the animal heme peroxidase superfamily. In particular, thermodynamic data of MPO will be presented and compared with the corresponding data of representatives of classes I (*20*), II (*21*), and III (*17*) of the bacterial, fungal, and plant heme peroxidase superfamilies, which do not have covalently bound heme. Significant differences have been found and are discussed with respect to the unique catalytic properties of MPO as well as its physiological relevance.

MATERIALS AND METHODS

Highly purified MPO with a purity index (A_{430}/A_{280}) of at least 0.85 was obtained from Planta Natural Products (http://www.planta.at). Its actual concentration was determined spectrophotometrically by using an ϵ_{430} of 91 000 M^{-1} cm^{-1} $heme^{-1}$ (*22*). All chemicals were reagent grade.

Spectroelectrochemistry. All experiments were carried out in an OTTLE cell assembled in our laboratory (*17*, *19*−*21*). The three-electrode configuration consisted of a gold minigrid working electrode (Buckbee-Mears, Chicago, IL), a homemade Ag/AgCl/KCl_{sat} microreference electrode, separated from the working solution by a Vycor set, and a platinum wire as the counter electrode. The reference electrode was calibrated against a saturated calomel electrode before each set of measurements. All potentials are referenced to the SHE. Potentials were applied across the OTTLE cell with an Amel model 2053 potentiostat/galvanostat. The functioning of the OTTLE cell was checked by measuring the reduction potential of yeast iso-1-cytochrome *c* under

conditions similar to those used in this work (*20*). The $E^{\circ\prime}$ value corresponded to that determined by cyclic voltammetry (260 mV). The constant temperature was maintained by a circulating water bath, and the OTTLE cell temperature was monitored with a Cu-costan microthermocouple. UV−vis spectra were recorded using a Varian Cary C50 spectrophotometer.

The variable-temperature experiments were performed using a "non-isothermal" cell configuration. The temperature of the reference electrode and the counter electrode was kept constant, while that of the working electrode was varied. For this experimental configuration, $\Delta S^{\circ\prime}_{rc}$ is calculated from the slope of the $E^{\circ\prime}$ versus temperature plot, whereas $\Delta H^{\circ\prime}_{rc}$ is obtained from the Gibbs−Helmholtz equation $\Delta G'^{\circ}_{rc} = \Delta H^{\circ\prime}_{rc} - T\Delta S^{\circ\prime}_{rc} = -nFE^{\circ\prime}$, namely from the slope of the $E^{\circ\prime}/T$ versus $1/T$ plot (*23*). The Faraday constant, F, is 96485.31 C/mol, and n represents the number of electrons transferred by the redox couple.

The spectroelectrochemical experiments on free MPO and on its cyanide adduct were carried out under argon from 10 to 45 °C, in the presence of 20 μM *N*,*N*,*N*′,*N*′-tetramethylphenylendiamine, 2-hydroxy-1,4-naphthoquinone, phenazine methosulfate, and phenazine ethosulfate used as mediators (*14*). In the former case, 1 mL samples containing 9.5 μM MPO made up in 0.1 M phosphate buffer and 0.1 M NaCl (pH 7) were used, whereas with the cyanide adduct, 1 mL samples containing 23 μM ARP and 2 mM potassium cyanide made up in 0.1 M phosphate buffer (pH 7) were employed.

Nernst plots consisted of at least five points and were invariably linear, with a slope consistent with a one-electron reduction process.

Application of conventional diffusion-controlled voltammetric techniques to MPO was hampered by its high molecular mass of 140 kDa.

RESULTS AND DISCUSSION

The spectroscopic properties of ferric and ferrous MPO and the corresponding cyanide adducts were similar to those reported in the literature (*11*). At pH 7.0, reduction of the Fe(III)−MPO complex (Soret band at 430 nm, Q-band at 570 nm, and CT band at 624 nm) gives a red-shifted spectrum with maxima at 473 and 638 nm. The corresponding cyanide complexes have their absorbance maxima at 455 and 634 nm [Fe(III)−CN] and 463 and 615 nm [Fe(II)−CN], respectively.

The electronic spectra of ferric high-spin MPO measured at different applied potentials in the OTTLE cell are shown in Figure 2A. The reduction potential of MPO (5 mV at 25 °C and pH 7.0) (Table 1) is somewhat lower than a previous literature value (21 mV) (*14*), probably as a consequence of differences in the ionic composition of the protein solutions that were employed. In any case, the obtained $E^{\circ\prime}$ value underlines the anomaly of MPO compared to homologous members of the animal peroxidase superfamily. In LPO, the determined value of the Fe(III)/Fe(II) couple is 195 mV lower than in MPO (*12*), which demonstrates the effect of modification and distortion of the heme as well as its immediate surrounding polypeptide matrix on the iron redox chemistry and, finally, reactivity. For EPO and TPO, no reduction potentials are reported, but given the high degree of similarity at the active site (*6*), it is reasonable to assume that they resemble LPO.

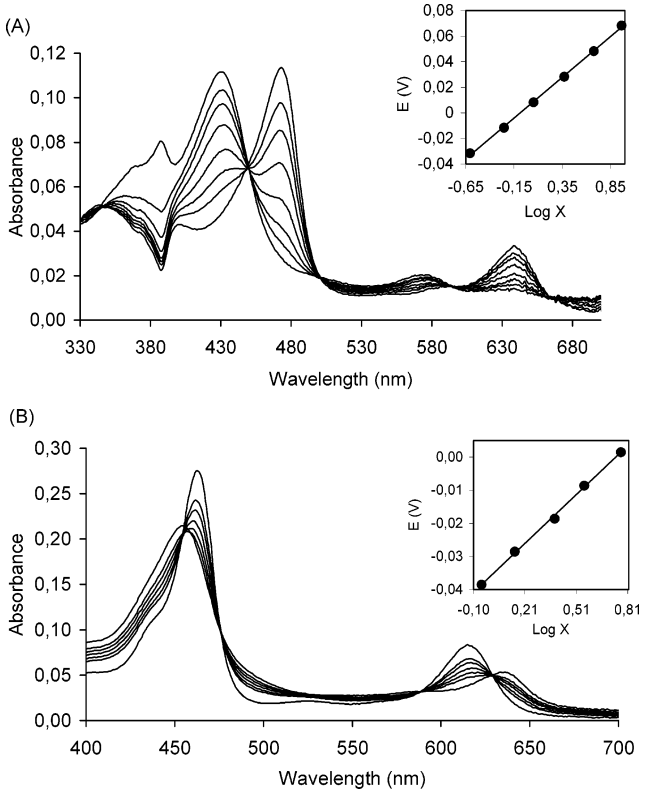

FIGURE 2: Electronic spectra of high-spin MPO (A) and its cyanide complex (B) obtained at various potentials. Spectra were recorded at 20 °C. The insets depict the corresponding Nernst plots, where X represents $(A_{\lambda_{red}^{max}} - A_{\lambda_{red}})/(A_{\lambda_{ox}^{max}} - A_{\lambda_{ox}})$ and $\lambda_{ox} = 430$ (A) or 634 nm (B) and $\lambda_{red} = 473$ (A) or 615 nm (B).

Table 1: Thermodynamic Parameters for the Fe(III) → Fe(II) Transition in Human Myeloperoxidase (MPO) in Its Resting State and in Its Cyanide Adduct[a]

ferric peroxidase	$E^{\circ\prime}$ (V)[b]	$\Delta H^{\circ\prime}_{rc}$ (kJ/mol)	$\Delta S^{\circ\prime}_{rc}$ (J K^{-1} mol^{-1})	$-\Delta H^{\circ\prime}_{rc}/F$ (V)	$T\Delta S^{\circ\prime}_{rc}/F$ (V)
MPO	**0.005**	**3**	**10**	**−0.031**	**0.031**
KatG (*20*)	−0.226	17	−18	−0.176	−0.056
ARP (*21*)	−0.183	−18	−120	0.187	−0.371
HRP-C (*17*)	−0.306	91	210	−0.943	0.648
MPO−CN	**−0.037**	**0**	**−12**	**0**	**−0.037**
ARP−CN (*21*)	−0.390	61	78	−0.632	0.241
HRP-C−CN (*17*)	−0.430	50	30	−0.517	0.093

[a] For comparison, the thermodynamic parameters of representatives of the three classes of the plant-type heme peroxidase superfamily are presented: class I (catalase peroxidase, KatG), class II (*A. ramosus* peroxidase, ARP), and class III (horseradish peroxidase isoform C, HRP-C). Average errors for $E^{\circ\prime}$, $\Delta H^{\circ\prime}_{rc}$, and $\Delta S^{\circ\prime}$ are ±0.005 V, ±4 kJ/mol, and ±8 J K^{-1} mol^{-1}, respectively. [b] At 298.15 K and termed the SHE. The sum $(-\Delta H^{\circ\prime}_{rc}/F + T\Delta S^{\circ\prime}_{rc}/F)$ often does not exactly match $E^{\circ\prime}$ since the $\Delta H^{\circ\prime}_{rc}$ and $\Delta S^{\circ\prime}_{rc}$ values are rounded to the closest integer, as a result of experimental error.

Table 1 shows that the $E^{\circ\prime}$ value of the Fe(III)/Fe(II) couple of LPO is in the range of plant-type peroxidases. In the latter enzyme superfamily, it is generally assumed that the Asp−His−iron interaction at the proximal heme side mainly contributes to $E^{\circ\prime}$ by deprotonating the N^{δ} position of the proximal histidine. In all animal peroxidases, the proximal histidine is hydrogen bonded to an asparagine. In MPO and LPO, both the orientation of the proximal histidine and the distance between the heme iron and its N^{ϵ} position

are very similar (≈2.2 Å). A significant difference exists in the distance between the N^{δ} position of His336 and the carbonyl oxygen of the amide group of Asn421. In MPO (2.9 Å), the distance is much longer than in LPO (2.6 Å), suggesting a higher imidazolate character of the proximal histidine in the latter metalloprotein. The effect seems to be enhanced by a closer contact of the guanidinium group of Arg333 with Asn421 in LPO compared to that in MPO. These structural features will contribute to some extent to the more positive reduction potential in MPO. The surroundings of the heme propionate groups are similar in both enzymes, but generally, the contacts between the propionate group on pyrrole ring D and the guanidinium groups of Arg424 and Arg333 are shorter in LPO. In both proteins, the ring C propionate interacts with conserved Asp98 and Thr100. The distance between the propionate oxygen and the Thr100 peptide NH group is again shorter in LPO. The extent of the influence of this more compact structure at the proximal heme side in LPO on the observed differences in $E^{\circ\prime}$ compared with MPO is not clear at the moment.

A major contribution to the $E^{\circ\prime}$ value in MPO may be the positive charge of the sulfur atom in the sulfonium ion linkage, which does not appear to be involved in any additional electrostatic interactions with the protein (*4*, *5*). The presence of such an electron-withdrawing group strongly influences the basicity of the four pyrrole nitrogens and thus decreases the electron density at the heme iron. Moreover, because of the distortions to the porphyrin ring, the iron in the high-spin state is positioned ~0.2 Å to the proximal side, which further reduces the contacts with the pyrrole nitrogens. Except for the sulfonium ion linkage in MPO, the distal heme cavity is similar in both proteins and occupied by the side chains of Gln91, His95, and Arg239. In both proteins, a water molecule (W1 in Figure 1B), which is hydrogen bonded to N^{ϵ} of the distal histidine, lies approximately midway between N^{ϵ} of His95 and Fe(III). The distance to Fe(III) in MPO and LPO is 3.0 and 2.6 Å, respectively. By all accounts, it seems to be the MPO-typical sulfonium ion linkage that primarily contributes to its peculiar redox behavior. The contribution of heme distortion *per se* to $E^{\circ\prime}$ is unknown.

To gain more insight into the mechanism of $E^{\circ\prime}$ modulation, we further investigated the temperature dependence of the reduction potential (Figure 3). This, performed for the first time for an animal peroxidase, allows factorization of the corresponding enthalpic and entropic components ($-\Delta H^{\circ\prime}_{rc}/F$ and $T\Delta S^{\circ\prime}_{rc}/F$). In MPO, the oxidized state is much less enthalpically stabilized compared with plant-type peroxidases. Interestingly, the enthalpy and entropy changes fully compensate. Hence, the two redox states of MPO exhibit the same thermodynamic stability at pH 7.0. As Table 1 underlines, in this respect, MPO is a unique heme peroxidase.

It has been shown that $\Delta H^{\circ\prime}_{rc}$ is determined primarily by metal−ligand binding interactions and the electrostatics at the interface among the metal, the protein environment, and the solvent (*16*). In plant-type peroxidases, the large enthalpic term that contributes to the stabilization of the ferric form (Table 1) has been attributed to the basic character of the proximal histidine, which stabilizes the higher oxidation state of the peroxidase, and to the polarity of the distal heme site maintained by the presence of water molecules involved in an extended network of hydrogen bonds (*17*). In MPO, the weaker imidazolate character of the proximal histidine, compared for example to that of HRP or LPO, and the electron withdrawing effect the sulfonium group connecting Met243 and the β-carbon of the vinyl group on pyrrole ring A reduce the electron density at the heme iron, thereby weakening the enthalpic stabilization of the ferric form of the enzyme due to ligand binding effects.

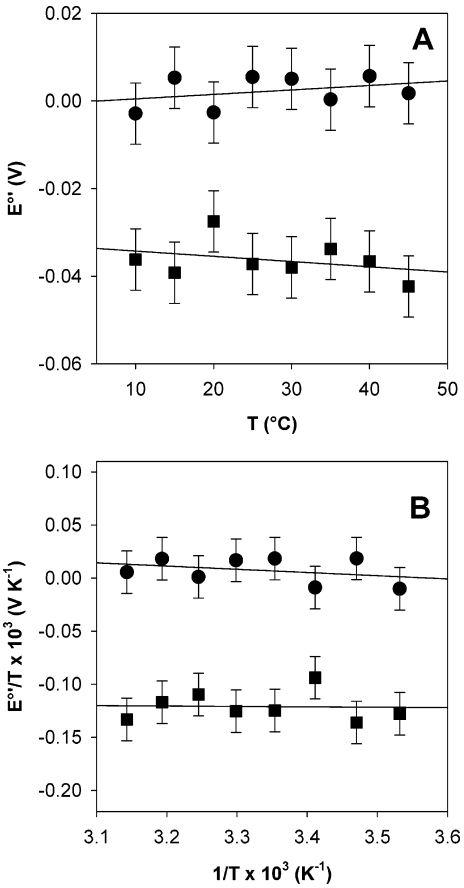

FIGURE 3: Temperature dependence of the reduction potential (A) and $E^{\circ\prime}/T$ vs $1/T$ plots (B) for human MPO (●) and its six-coordinate cyanide adduct (■). The slopes of the plots yield $\Delta S^{\circ\prime}_{rc}/F$ and $-\Delta H^{\circ\prime}_{rc}/F$ values, respectively.

In MPO, the distal heme cavity is also filled with water molecules that are hydrogen bonded to Gln91, His95, and Arg239 (Figure 1) and to each other and fill a funnel-shaped channel leading from the distal cavity to the surface of the protein (*4*). Compared to plant-type peroxidases, the water molecule closest to the metal is farther from Fe(III) which could induce a different H-bonding pattern and a lower polarity. It has been suggested that these factors contribute to differences in $E^{\circ\prime}$ between HRP and ARP (*17*, *21*).

In ET metalloproteins and redox metalloenzymes, $\Delta H^{\circ\prime}_{rc}$ and $\Delta S^{\circ\prime}_{rc}$ are composed of protein intrinsic contributions [$\Delta H^{\circ\prime}_{rc(int)}$ and $\Delta S^{\circ\prime}_{rc(int)}$, the latter of which depends on protein conformational factors] and solvent reorganization factors [$\Delta H^{\circ\prime}_{rc(solv)}$ and $\Delta S^{\circ\prime}_{rc(solv)}$] (*19*, *21*):

$$\Delta H^{\circ\prime}_{rc} = \Delta H^{\circ\prime}_{rc(int)} + \Delta H^{\circ\prime}_{rc(solv)}$$

$$\Delta S^{\circ\prime}_{rc} = \Delta S^{\circ\prime}_{rc(int)} + \Delta S^{\circ\prime}_{rc(solv)}$$

Though the structural changes of MPO upon reduction are not documented by a structure of ferrous MPO, on the basis of the known structures (*4*, *5*) of the MPO−bromide, MPO−

thiocyanate, and MPO−cyanide complexes, which exhibit relatively small conformational changes compared to ferric MPO, it is reasonable to attribute, to a first approximation, the measured changes in reaction entropy only to the effects of reduction-induced solvent reorganization, thus neglecting protein-based factors related to differences in conformational degrees of freedom [$\Delta S^{\circ\prime}_{rc(int)} \approx 0$]:

$$\Delta S^{\circ\prime}_{rc} = \Delta S^{\circ\prime}_{rc(solv)}$$

In the case of HRP, it has been demonstrated that this approach is rational since electron uptake of ferric HRP induced only a very limited change in the overall protein structure (*21*, *24*, *25*). Moreover, reduction-induced solvent reorganization effects (e.g., changes in the H-bonding network involving the water molecules within the hydration sphere of the protein) have been found to induce compensatory enthalpy and entropy changes (*26*−*29*):

$$\Delta H^{\circ\prime}_{rc(solv)} = T\Delta S^{\circ\prime}_{rc(solv)}$$

Therefore, the corresponding enthalpic contribution can be factorized out of the measured enthalpy change, finally allowing estimation of the intrinsic contribution:

$$\Delta H^{\circ\prime}_{int} = \Delta H^{\circ\prime}_{rc} - \Delta H^{\circ\prime}_{rc(solv)} = \Delta H^{\circ\prime}_{rc} - T\Delta S^{\circ\prime}_{rc(solv)} \approx 0$$

In the case of MPO, this underlines the fact that the small enthalpic effect that slightly stabilizes ferric MPO is only due solvent reorganization effects, whereas in plant-type peroxidases, protein intrinsic factors also contribute to the stabilization of the enzymes in the Fe(III) state (*17*, *21*).

The absolute value of $\Delta S^{\circ\prime}_{rc}$ of MPO is sensibly smaller than those of HRP and ARP (Table 1), indicating much smaller reduction-induced solvent reorganization effects than in the latter enzymes. This is in agreement with the impression of an increased rigidity of the hydrogen bond network involving the water molecules in the substrate channel leading to the distal heme site, afforded by the analysis of the three-dimensional structure of native MPO and of its adducts with bromide, thiocyanate, and cyanide (*4*, *5*). This difference is quite intriguing and can be functionally relevant. In fact, a low mobility of the water molecules in the heme distal cavity could be crucial in fixing the position of the chloride ion to be oxidized through electrostatic interactions, as indicated by the structure of the MPO−bromide and MPO−bromide−cyanide adducts (*5*), and in helping in the transfer and incorporation of the oxyferryl oxygen into HClO (*30*). This feature is not crucial in HRP and ARP, since they simply extract electrons from their aromatic substrates (which do not enter into the heme cavity), without oxygen atom transfer (*11*).

Furthermore, we have determined the reduction potential of the cyanide adduct of MPO to be −37 mV at 25 °C and pH 7.0 (Figure 2B). This is the only $E^{\circ\prime}$ value available for a member of the animal peroxidase superfamily in its low-spin form. Comparison with plant-type peroxidases clearly shows (Table 1) that the difference in $E^{\circ\prime}$ values between high-spin MPO and MPO−CN is small (42 mV) compared with that of ARP (207 mV) or HRP-C (124 mV). The slightly negative value of $E^{\circ\prime}$ turned out to be fully the result of an entropic contribution that disfavors Fe(III) reduction (Table 1), in contrast with plant-type peroxidases, whose six-coordinated low-spin CN adducts are characterized by positive reduction enthalpies and entropies (Table 1) (*17*, *19*−*21*).

The structure of the MPO−cyanide complex (*5*) shows that there are no significant conformational changes associated with cyanide binding. During the transition from the high-spin ($S = {}^5/_2$) to the low-spin ($S = {}^1/_2$) form, the iron slightly shifts into the heme plane and the bound cyanide displaces water W1 (Figure 1C,D). The iron−cyanide carbon distance of 2.1 Å is shorter than the distance of 3 Å between the oxygen of W1 in the high-spin protein, and cyanide is inclined toward W2 and W3 (Figure 1C). Water molecule W2 shifts slightly away from the cyanide nitrogen, but a compensatory shift in W5 maintains the hydrogen bonding between these water molecules. No other solvent reorganization effects are obvious from the structure of the MPO−cyanide complex. Taken together, the structural changes are restricted to the immediate heme surroundings and are small. When cyanide binds, the immediate heme iron environment becomes more compact without influencing the H-bonding network in the substrate channel. Normally, in the Fe(II) form of heme proteins, the electrostatic interaction of the metal ion with the water molecules in the heme cavity is weakened compared to that in the ferric form, lowering the order of their arrangement. This effect is much smaller in the corresponding cyanide complexes, where the accessibility to the heme is diminished. Due to the lower polarity in the high-spin state as well as due to the presence of the sulfonium ion linkage also in the Fe(II) form, the effect of spin change in MPO on $\Delta S^{\circ\prime}$ is small. Since $\Delta H^{\circ\prime}_{rc} \approx 0$, it follows that the protein intrinsic factors and solvent reorganization factors either offset [$\Delta H^{\circ\prime}_{rc(int)} = -\Delta H^{\circ\prime}_{rc(solv)}$] or are negligibly small ($\approx$0).

In conclusion, MPO exhibits extraordinary redox properties that distinguish this heme enzyme from other peroxidases and reflect its physiological role in the innate immune defense system. It has a hemoglobin-like reduction potential of the Fe(III)/Fe(II) couple, and both redox states exhibit the same thermodynamic stability at pH 7.0. As a consequence, ferrous MPO must be taken into account when considering enzyme mechanisms. Ferrous MPO is outside of both the peroxidase and halogenation cycle (*6*) but can react with hydrogen peroxide or molecular oxygen to compound II (*31*) or compound III (*32*), the latter being a ferrous−dioxy/ferric superoxide complex similar to oxyhemoglobin or oxymyoglobin, and decays to ferric MPO. This peculiar redox behavior, which is not typical for a heme peroxidase, is the consequence of its physiological role. To oxidize chloride, it is necessary that the higher oxidation states (e.g., compound I) also have a very positive reduction potential. The only way is to decrease the electron density at the heme iron by (i) lowering the basicity of the proximal ligand, (ii) lowering the basicity of pyrrole nitrogens of the porphyrin by including strong electron-withdrawing groups, (iii) offering charged groups around the redox site, and/or (iv) heme distortion that favors a pronounced out-of-plane structure of the iron ion. Myeloperoxidase is an excellent model that demonstrates the effect of these modifications on the redox properties of all relevant couples, i.e., Fe(III)/Fe(II), compound I/Fe(III), and compound I/compound II.

REFERENCES

1. Klebanoff, S. J. (2005) Myeloperoxidase: Friend and foe, *J. Leukocyte Biol. 77*, 598−625.
2. Taurog, A. (1999) Molecular evolution of thyroid peroxidase, *Biochimie 81*, 557−562.
3. Arnhold, J., Furtmüller, P. G., and Obinger, C. (2003) Redox properties of myeloperoxidase, *Redox Rep. 8*, 179−186.
4. Fiedler, T. J., Davey, C. A., and Fenna, R. E. (2000) X-ray crystal structure and characterization of halide-binding sites of human myeloperoxidase at 1.8 Å resolution, *J. Biol. Chem. 275*, 11964−11971.
5. Blair-Johnson, M., Fiedler, T., and Fenna, R. E. (2001) Human myeloperoxidase: Structure of a cyanide complex and its interaction with bromide and thiocyanate substrates at 1.9 Å resolution, *Biochemistry 40*, 13990−13997.
6. Furtmüller, P. G., Zederbauer, M., Jantschko, W., Helm, J., Bogner, M., Jakopitsch, C., and Obinger, C. (2006) Active site structure and catalytic mechanisms of human peroxidases, *Arch. Biochem. Biophys. 445*, 199−213.
7. Newton, N., Morell, D. B., and Clarke, L. (1965) The haem prosthetic groups of some animal peroxidases. II. Myeloperoxidase, *Biochim. Biophys. Acta 96*, 476−486.
8. Wever, R., and Plat, H. (1981) Spectral properties of myeloperoxidase and its ligand complexes, *Biochim. Biophys. Acta 661*, 235−239.
9. Kooter, I. M., Moguilevsky, N., Bollen, A., Sijtsema, N. M., Otto, C., and Wever, R. (1997) Site-directed mutagenesis of Met243, a residue of myeloperoxidase involved in binding of the prosthetic group, *J. Biol. Inorg. Chem. 2*, 191−196.
10. Brogioni, S., Feis, A., Marzocchi, M. P., Zederbauer, M., Furtmüller, P. G., Obinger, C., and Smulevich, G. (2006) Resonance Raman assignment of myeloperoxidase and selected mutants Asp94Val and Met243Thr. Effect of the heme-distortion, *J. Raman Spectrosc. 37*, 263−276.
11. Dunford, H. B. (1999) *Heme peroxidases*, Wiley-VCH, New York.
12. Ohlsson, P. I., and Paul, G. (1983) The reduction potential of lactoperoxidase, *Acta Chem. Scand. 37*, 917−921.
13. Harrison, J. E., and Schultz, J. (1978) Myeloperoxidase: Confirmation and nature of heme-binding inequivalence: Resolution of a carbonyl-substituted heme, *Biochim. Biophys. Acta 536*, 341−346.
14. Ikeda-Saito, M., and Prince, R. C. (1985) The effect of chloride on the redox and EPR properties of myeloperoxidase, *J. Biol. Chem. 260*, 8301−8305.
15. Bertrand, P., Mbarki, O., Asso, M., Blanchard, L., Guerlesquin, F., and Tegoni, M. (1995) Control of the redox potential in *c*-type cytochromes: Importance of the entropic contribution, *Biochemistry 34*, 11071−11079.
16. Battistuzzi, G., Borsari, M., Cowan, J. A., Ranieri, A., and Sola, M. (2002) Control of Cytochrome c Redox Potential: Axial Ligation and Protein Environment Effects, *J. Am. Chem. Soc. 124*, 5315−5324.
17. Battistuzzi, G., Borsari, M., Ranieri, A., and Sola, M. (2002) Redox thermodynamics of the Fe^{3+}/Fe^{2+} couple in horseradish peroxidase and its cyanide complex, *J. Am. Chem. Soc. 124*, 26−27.
18. Kadish, K. M., Thompson, L. K., Beroiz, D., and Bottomley, L. A. (1977) in *Electrochemical studies of biological systems* (Sawyer, D. T., Ed.) ACS Symposium Series 38, American Chemical Society, Washington, DC.
19. Battistuzzi, G., Bellei, M., Borsari, M., Di Rocco, G., Ranieri, A., and Sola, M. (2005) Axial ligation and polypeptide matrix effects on the reduction potential of heme proteins probed on their cyanide adducts, *J. Biol. Inorg. Chem. 10*, 643−651.
20. Bellei, M., Battistuzzi, G., Jakopitsch, C., Sola, M., and Obinger, C. (2006) Redox thermodynamics of the ferric-ferrous couple of wild-type *Synechocystis* KatG and KatG(Y249F), *Biochemistry 45*, 4768−4774.
21. Battistuzzi, G., Bellei, M., De Rienzo, F., and Sola, M. (2006) Redox properties of the Fe^{3+}/Fe^{2+} couple in *Arthromyces ramosus* class II peroxidase and its cyanide adduct, *J. Biol. Inorg. Chem. 11*, 586.
22. Odajima, T., and Yamazaki, I. (1970) Myeloperoxidase of the leukocyte of normal blood. I. Reaction of myeloperoxidase with hydrogen peroxide, *Biochim. Biophys. Acta 206*, 71−74.
23. Yee, E. L., Cave, R. J., Guyer, K. L., Tyma, P. D., and Weaver, M. J. (1979) A survey of ligand effects upon the reaction entropies of some transition metal redox couples, *J. Am. Chem. Soc. 101*, 1131−1137.
24. Berglund, G. I., Carlsson, G. H., Smith, A. T., Szöke, H., Henriksen, A., and Hajdu, J. (2002) The catalytic pathway of horseradish peroxidase at high resolution, *Nature 417*, 463−468.
25. Carlsson, G. H., Nicholls, P., Svistunenko, D., Berglund, G. I., and Hajdu, J. (2005) Complexes of horseradish peroxidase with formate, acetate, and carbon monoxide, *Biochemistry 44*, 635−642.
26. Battistuzzi, G., Borsari, M., Di Rocco, G., Ranieri, A., and Sola, M. (2004) Enthalpy/entropy compensation phenomena in the reduction thermodynamics of electron transport metalloproteins, *J. Biol. Inorg. Chem. 9*, 23−26.
27. Canters, G. W., Kolczak, U., Armstrong, F., Jeuken, L. J. C., Camba, R., and Sola, M. (2000) The effect of pH and ligand exchange on the redox properties of blue copper proteins, *Faraday Discuss. 116*, 205−220.
28. Grunwald, E., and Steel, C. (1995) Solvent reorganization and thermodynamic enthalpy-entropy compensation, *J. Am. Chem. Soc. 117*, 5687−5692.
29. Liu, L., and Guo, Q.-X. (2001) Isokinetic relationship, isoequilibrium relationship, and enthalpy-entropy compensation, *Chem. Rev. 101*, 673−695.
30. Zederbauer, M., Jantschko, W., Neugschwandtner, M., Jakopitsch, C., Moguilevsky, N., Obinger, C., and Furtmüller, P. G. (2005) Role of the covalent glutamic acid 242-heme linkage in the formation and reactivity of redox intermediates of human myeloperoxidase, *Biochemistry 44*, 6482−6491.
31. Jantschko, W., Furtmüller, P. G., Zederbauer, M., Lanz, M., Jakopitsch, C., and Obinger, C. (2003) Direct conversion of ferrous myeloperoxidase to compound II by hydrogen peroxide: An anaerobic stopped-flow study, *Biochem. Biophys. Res. Commun. 312*, 583−592.
32. Jantschko, W., Furtmüller, P. G., Allegra, M., Livrea, M. A., Jakopitsch, C., Regelsberger, G., and Obinger, C. (2002) Redox intermediates of plant and mammalian peroxidases: A comparative transient-kinetic study of their reactivity toward indole derivatives, *Arch. Biochem. Biophys. 398*, 12−22.

BI061647K